

## THERMAL EVOLUTION OF A SLATE

P. J. Sánchez-Soto<sup>1\*</sup>, A. Ruiz-Conde<sup>1</sup>, R. Bono<sup>1</sup>, M. Raigón<sup>2</sup> and E. Garzón<sup>3</sup>

<sup>1</sup>Instituto de Ciencia de Materiales de Sevilla (ICMSE), Centro Mixto Consejo Superior de Investigaciones Científicas (CSIC) – Universidad de Sevilla, c/Américo Vespucio 49, Isla de la Cartuja, 41092 Sevilla, Spain

<sup>2</sup>Departamento de Ingeniería Mecánica y de los Materiales, Escuela Superior de Ingenieros, Universidad de Sevilla, 41092 Sevilla, Spain

<sup>3</sup>Departamento de Ingeniería Rural, Universidad de Almería, La Cañada de San Urbano, 04120 Almería, Spain

The thermal evolution of a slate rock sample (Berja, Almería, Spain) has been studied. The phase minerals identified in this sample were mica (illite), chlorite (clinochlore) and quartz as major components, with minor microcline, iron oxide and a mixed-layer or interstratified phase (montmorillonite-chlorite). This slate is highly silico-aluminous (48.33 mass% silica, 22.04 mass% alumina), and ca. 20 mass% of other elements, mainly Fe<sub>2</sub>O<sub>3</sub> (8.35 mass%), alkaline-earths and alkaline oxides.

Two main endothermic DTA effects, centered at 640 and 730°C, were observed. The more important contribution of total mass loss (7.15 mass%) was found between 500–900°C, with two DTG peaks detected at 630 and 725°C. All these effects were associated to the dehydroxylation of structural OH groups of 2:1 layered silicates mixed in the slate. The dehydroxylation of the layered silicates evidenced by dilatometry, produced a rapid increase of expansion between 600–800°C. The thermal evolution of the slate upper 800°C indicated the first sintering effects associated to shrinkage, which is also favoured by its low particle size (average 23 µm) and the presence of a liquid or vitreous phase as increasing the heating temperature. The application of thermal diffractometry to the slate sample allowed to study the formation of dehydroxylated crystalline phases from the layered silicates after heating. At 1000°C, β-quartz, dehydroxylated illite, iron oxide, relicts of microcline and the vitreous phase were present in the sample. All these results are interesting to know the thermal behaviour of a complex mineral mixture as identified in the slate.

**Keywords:** chlorite, dehydroxylation, dilatometry, DTA-TG, illite, interstratified phase, slate, thermal diffractometry

### Introduction

Slates are rocks constituted mainly by layered minerals, such as illite, kaolinite and chlorite, besides quartz. Other minerals can be present in low proportion, such as feldspars, carbonates (calcite, dolomite), iron oxide and sulfides [1–9]. They are considered as compacted metamorphic rocks of fine grain characterized by slaty cleavage [3–5]. According to an industrial description [6], slate is a sedimentary derivation rock with fine granulation, weakly metamorphized, characterized by perfect cleavage, thus being able to form big sheets of just a few millimeters in thickness, in a continuous flat surface. Its physical properties, such as preferential cleavage, average hardness, low porosity, high mechanical resistance of its composing minerals to bad weather, etc., allow for its utilization as revestments in various areas of building construction and architecture (floor tiles, slabs, roof tiles) with the shape of plates because they are resistant, unchanging, insulating and waterproof. High-quality slates used as ornamental rocks show a low porosity and water absorption capacity, very low thermal and electrical conductivity and relative high resistance at temperature changes [7–13]. The colour of the slates can be violet, gray, beige, redish, green and black [6, 7, 13].

They can be also applied in paving roads, cement fabrication, as fillers in plastics and paintings, and as carrier in agriculture, being a raw material for the preparation of lightweight aggregates for concrete after firing (~1200–1500°C) resulting a very porous material [2, 7–9, 13, 14]. The wastes of slate processing are interesting for new and interesting applications, for instance in the fabrication of materials such as the ceramic foams with low mass, low density and low thermal conductivity [10–13, 15]. The ceramic foams have useful applications, such as high-temperature filters, thermal barriers and lightweight structures [15].

There are several studies on thermal behaviour of slates with a particular mineralogy composition [8, 11, 15–20]. These investigations attempt to describe the complex thermal transformations of the phase minerals that constitute the slate. For instance, Rodríguez *et al.* [8] studied a slate sample (Badajoz, Spain) containing mainly quartz and, in less proportion, muscovite, chlorite and feldspar, with secondary minerals like pyrite, hematite and goethite. These authors reported that chlorite disappears at 800°C by thermal treatment of the slate, muscovite is slightly modified and quartz is undranged, being this process exothermic in accordance with their results obtained by DTA [8]. Cambronero *et al.* [15] investigated

\* Author for correspondence: pedroji@icmse.csic.es

a slate sample (Orense, Spain) containing quartz, muscovite (sericite), chlorite, kaolinite, feldspars, calcite, pyrite and carbonaceous matter (graphite). In a study on Spanish roofing slate deposits, Garcia-Guinea *et al.* [16] claimed that Spain is the first country in world production of slate roofs. The same research group studied the thermal and optical behaviour of a slate (Orense, Spain) used in building construction [17]. In a further study on this slate, Garcia-Guinea *et al.* [18] examined the dehydroxylation and the Ostwald ripening effects [19].

The aim of the present paper is to study the thermal behaviour of a slate sample. It was interesting to investigate this slate using thermal methods because: (a) at the present, there are scarce studies on this material [21] and (b) to relate the results with those reported previously on other slate samples. This study is a part of a research program on new deposits of slates in SW Spain (Granada and Almería) as raw materials for new and improved applications. The knowledge of mineralogy and physicochemical characteristics will be worth to differentiate several slate deposits. Large amounts of slates from Berja have been traditionally used as impermeabilization materials for roofs, beds and ponds. These slates have been even processed as compacted powders after grinding the raw material. On the basis of the research results, new applications would be proposed.

## Experimental

### Sample

The original compacted slate samples in fragments (5–7 kg) were obtained at the deposit of Berja (Almería, SW Spain). They show a gray colour, a greasy touch and slaty cleavage. These samples were crushed, lightly ground and sieved to pass 63  $\mu\text{m}$  to obtain a representative and more homogeneous sample. This powdered sample was dried at 110°C during 24 h. Aliquots of dried sample (1–2 g) were gently ground using an agate mortar for further analysis using several techniques.

### Analytical techniques

Chemical analysis was performed by X-ray fluorescence (XRF) using a sequential Bruker SRS-3000 spectrometer with Rh X-ray tube. Cylindrical pressed samples were prepared using a laboratory press.

The particle size analysis of the sample lightly ground and sieved to pass 100  $\mu\text{m}$  was performed by a wet aqueous method previously applied in layered silicates [22], using a Mastersizer X Laser equipment of Malver Instruments.

Differential thermal analysis (DTA) and thermogravimetric (TG) curves were obtained in air flow (400 mL  $\text{min}^{-1}$ ) using a thermal analyzer system TG/DTA 6300 Seiko Instruments, model EXSTAR 6000. The heating rate was 10°C  $\text{min}^{-1}$  up to 1000°C. Calcined alumina was used as the reference material and Pt–Pt/Rh 13% thermocouples. Samples of 26 mg exactly weighed were gently packed into cylindrical Pt crucibles.

The total mass loss (average of three measurements) was also determined using 1.0000 g of sample after heating into a Hobersal ceramic furnace, model HD-230, up to 1000°C, with 1 h of holding time.

The contraction-expansion behaviour of the slate was investigated up to 1100°C using a Setaram Setsys dilatometer, model TMA-18, with alumina probe and cylindrical pressed samples of 4.05 mm height, at a heating rate of 6°C  $\text{min}^{-1}$ .

X-ray powder diffraction diagrams (XRD) were obtained using a Bruker diffractometer, model D-501. The patterns in disoriented preparations were obtained with Ni-filtered  $\text{CuK}\alpha$  radiation, graphite monochromator, at 36 kV and 26 mA and scanning speed of 1° in  $2\theta$   $\text{min}^{-1}$ . The identification of crystalline phases was performed using a software program, available with the equipment, and a SICOMP PC 16-20 system, taking into account the Joint Committee For Powder Diffraction Standards (JCPDS) files. Thermal diffractometry from room temperature up to 1000°C was also applied to study the thermal evolution of the slate sample. The equipment was a Philips X'Pert diffractometer using Ni-filtered  $\text{CuK}\alpha$  radiation, at 40 kV and 40 mA, with a scanning speed of 0.05° in  $2\theta$   $\text{s}^{-1}$  from 5 to 80°  $2\theta$  and  $\theta$ – $\theta$  goniometer, with detector X'Celerator. The XRD runs were performed each 50°C of heating in static air. The high-temperature camera with temperature-controlled device was Anton Paar HTK 1200.

## Results and discussion

Figure 1 shows the XRD pattern of the powdered slate sample. The crystalline phase composition deduced from X-ray study was mica (muscovite or illite), and chlorite, both layered silicates, quartz and minor feldspars (microcline) and iron oxide. These minerals correspond to a common slate sample [1–9]. The identification of the crystalline phases was carried out by their characteristic patterns [23]. A semiquantitative assessment of the mineralogical composition (in mass%) of the slate sample, as a bulk, gave average figures of 50–60% mica, 20–15% quartz, 10–15% chlorite, 5–10% feldspars (microcline) and ca. 5% iron oxide. The presence of chlorite was confirmed using the treatments to differentiate it from kaolinite [24].

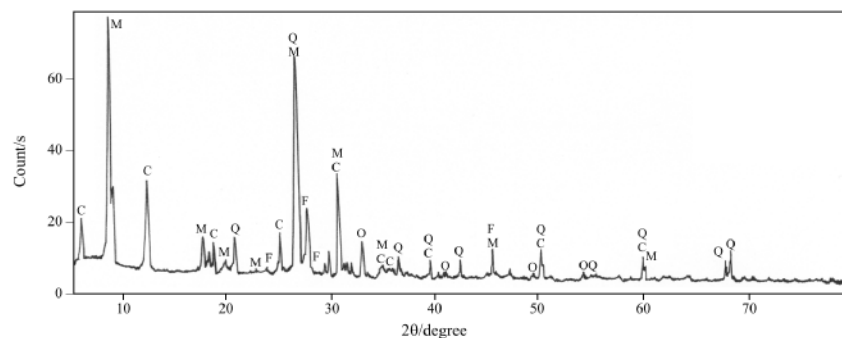


**Fig. 1** XRD powder diagram of the slate sample. The main crystalline phase minerals identified are M=mica (muscovite, illite), C=chlorite (clinochlore), Q=quartz, F=K-feldspar (microcline) and O=iron oxide. Mica muscovite, JCPDS card 7-0042 and chemical composition  $(K,Na)(Al,Mg,Fe)_2Si_3Al_{0.9}O_{10}(OH)_2$ ; chlorite (clinochlore), JCPDS card 7-0078 and chemical composition  $(Mg,Fe,Al)_6(Si,Al)_4O_{10}(OH)_8$ ; quartz, JCPDS card 33-1161; feldspar (microcline), JCPDS card 2-0513 and chemical composition  $Al_2O_3K_2O_6SiO_2$ ; iron oxide, JCPDS card 5-0637 and chemical composition  $Fe_2O_3$

However, it is worth to note that further X-ray analysis revealed the presence of a mixed-layer or interstratified phase in this slate sample (Fig. 2). It can be thus seen that this interstratified phase would correspond to mixed-layer montmorillonite-chlorite. The presence of this kind of phase has not previously been reported in the literature concerning slates. Information on the types of layer present in mixed-layer minerals, their proportion, and the pattern of interstratification can be obtained directly from mathematical analysis of the positions and intensities of XRD basal reflections [25–27]. This complex analysis will be a matter of additional work [28]. It should be emphasized that the presence of interstratified phases would influence the thermal behaviour observed in mineral samples, as demonstrated in a previous paper [29].

On the other hand, the chemical composition of the slate sample is given in Table 1. Silica and alumina are the oxides with the highest percentages, which allows to qualify this sample as silico-aluminous. However, more than 20 mass% of the total chemical composition of the slate is formed by impurity oxides, in particular iron, alkaline-earths and alkaline oxides, which will form a vitreous or liquid phase by thermal

treatments [30]. The high value of silica is associated with the presence of free quartz, as found by XRD (Fig. 1). In general, the chemical data were in well agreement with the mineralogical composition determined by XRD. The  $K_2O$  content was associated with the presence of potassium mica (muscovite or illite) and potassium feldspar (microcline). The content of  $Fe_2O_3$  is 8.35 mass%, which can be associated to free iron oxide, besides the contribution of iron in the crystalline silicate structures. The same can be said for MgO content, mainly associated to clinochlore, and even CaO and  $Na_2O$  and the presence of exchangeable cations. In particular, part of CaO content could be also associated to the presence of interstratified montmorillonite-chlorite as a mineral phase (Fig. 2). Finally, the total mass loss at 1000°C must be associated to the dehydroxylation of layered silicates, which are present in major proportion.

In a previous study of slate samples, Cambronero *et al.* [15] have found similar results as shown in Table 1 concerning the chemical analysis of their sample. Their results (in mass%) have showed that  $Fe_2O_3$  is 9.95% and the mass loss after heating at 600°C ranges between 6.5–7.1%, although  $SiO_2$  content in that slate is slightly higher (54.68%) than

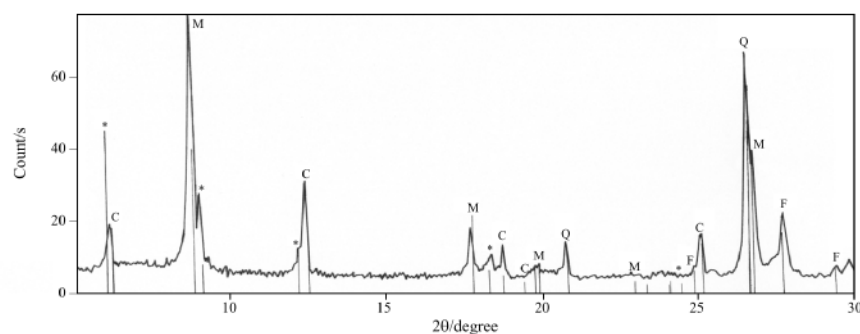


**Fig. 2** XRD powder diagram in the zone  $2\theta=5-30^\circ$  to identify the presence of a mixed-layer or interstratified phase montmorillonite-chlorite denoted by asterisks (\*), showing the relative intensities of each peak. Symbols meaning as in Fig. 1. Montmorillonite-chlorite, JCPDS card 7-0027 and chemical composition  $AlCaNaSi_4O_{11}$

**Table 1** Chemical analysis (mass%) by XRF of the slate sample

SiO <sub>2</sub>	Al <sub>2</sub> O <sub>3</sub>	Fe <sub>2</sub> O <sub>3</sub>	TiO <sub>2</sub>	CaO	MgO	Na <sub>2</sub> O	K <sub>2</sub> O	LOI*	Total
48.33	22.04	8.35	1.15	4.43	3.43	1.84	3.32	7.02	99.91

\*LOI = loss on ignition, total mass loss after heating at 1000°C for 1 h

the present results (Table 1), Al<sub>2</sub>O<sub>3</sub> is 23.52%, CaO is 0.54% and MgO is 3.75%, and the sum (Na<sub>2</sub>O+K<sub>2</sub>O) is 5.96%. These authors [15] identified muscovite (sericite), chlorite, kaolinite, quartz, calcite, feldspars, pyrite and graphite (powder <45 μm). However, they claimed that the chlorite mineral is chamosite, but no additional results to confirm it were reported. In other studies on slate samples, Rodriguez *et al.* [8, 9, 20] identified quartz, muscovite, chlorite and small amounts of feldspars, which correspond to a common slate. They reported similar chemical analysis results as compared to those presented in Table 1, with 6.72% Fe<sub>2</sub>O<sub>3</sub> and a mass loss after heating at 1000°C of 5.54%. The SiO<sub>2</sub> content is higher (58.77%) than the present results (Table 1). These authors found 20.95% Al<sub>2</sub>O<sub>3</sub>, 0.27% CaO and 1.87% MgO; the sum (Na<sub>2</sub>O+K<sub>2</sub>O) was 2.49%. However, the contribution of CaO in the present slate sample is more important than that found in precedent papers concerning chemical analysis data on slate samples. It is associated to the presence of the interstratified crystalline phase (Fig. 2), and probably in part as exchangeable cations. On the other hand, Rodriguez *et al.* [8, 9, 20] indicated that ‘the presence of magnesia suggest the mica nature of the slate sample’. This asseveration is not consistent with the mica muscovite that they identified by XRD in their slate sample.

Concerning the particle size of the slate sample studied in the present paper, it was found a high proportion of sample less than 100 μm (80 mass%). After sieving, the particle size analysis showed that the largest contribution of particle size distribution is between 1–100 μm. It was calculated an average particle size of 23 μm. Taking into account this result, the mica muscovite mineral identified by XRD (Fig. 1) might be considered as sericite or illite (naturally occurring clay-grade micas) [5]. The term ‘illite’ was proposed as a general term given to a mixture of minerals, including muscovite and feldspar, whose physical properties resemble those of the mica family [5]. It has been generally accepted that the main difference between mica and illite is that micas contain more potassium as interlayer cations, whereas illite contains more water and silica.

Figure 3 shows the DTA-TG curves for this slate sample. It can be observed two main endothermic DTA effects centered at 640 and 730°C (asymmetric) accompanied by mass losses between 500–900°C. They are associated to dehydroxylation and water elimination of structural OH groups of the layered

silicates, mainly chlorite and mica. The sharp endothermic DTA effect at 573°C corresponds to the quartz α→β phase transition. On the other hand, the total mass loss after dynamic heating of the slate sample is 7.15%, in good agreement with that reported in Table 1 (1000°C for 1 h). The first mass loss in the TG diagram calculated from room temperature up to ca. 200°C is very low (0.27%); the second one, from 200 up to 650°C, amounts 2.22%; the third mass loss, from 650°C up to ca. 770°C, amounts 4.14%; finally, there is a fourth mass loss from 770 to 1000°C which amounts 0.52%. The mass loss is almost constant above 900°C. Associated to these thermal changes, DTG curve shows two main peaks centered at ca. 630 and 725°C, the last of larger intensity.

Previous studies on thermal evolution of chlorites [31, 32] reported that the minerals of chlorite group present a typical DTA curve with an endothermic effect between 575–610°C and other one centered at 740°C. The first one is associated to dehydroxylation of brucite-like layers and the second one to dehydroxylation of mica or 2:1 talc-like sheet layers. However, in the present case, this second endothermic DTA effect is superposed with the endothermic effect of dehydroxylation of mica (muscovite or illite). This assumption explains the larger mass loss observed in the TG diagram of the slate sample above 600°C and the increase in intensity of DTG peak centered at 725°C. On the other hand, the dehydroxylation of mica (muscovite, illite) has been previously studied by several authors [33–38]. Several factors, such as particle size, time, temperature and structure of layer silicates, influence the thermal behaviour. It should be noted that chlorite and

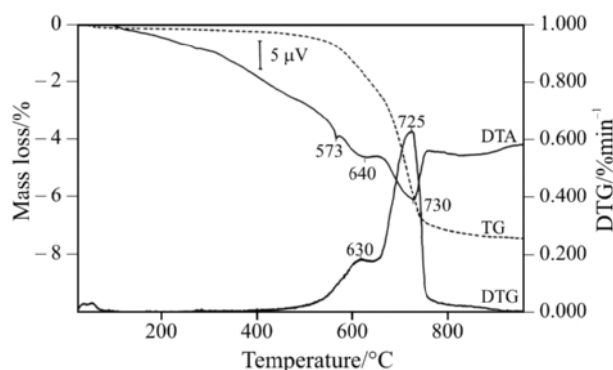


**Fig. 3** DTA-TG-DTG curves of the slate sample. The heating rate was 10°C min<sup>-1</sup> up to 1000°C in air flow (400 mL min<sup>-1</sup>), using calcined alumina as reference material and sample mass of 26 mg

mica (muscovite) are 2:1 layer type silicates [39]. The minerals of chlorite group are characterized by an additional brucite layer with subdivision in subgroups: di- and trioctahedric chlorites. Thus, clinocllore is associated to this last subgroup [39], being identified as the chlorite mineral present in the slate sample (Fig. 1). Illite has a 2:1 layer structure having a plane of octahedrally coordinated cations (gibbsite) sandwiched between 2 inward pointings sheets of tetrahedra (silica). Further discussion on the structure of 1:1 and 2:1 layer silicates and the interlayer material to understand their differences in thermal stability and decomposition is included in [40]. In general, the thermal analysis by DTA-TG (Fig. 3) confirmed the mineral phase composition of this slate sample as found by XRD (chlorite, mica and quartz). However, the presence of mineral interstratified phases influences the thermal behaviour, as found in a previous paper on layered silicates [29].

Dilatometric analysis of this slate sample (Fig. 4, curve a) shows a slow and continuous expansion by dynamic heating up to ca. 400°C, with constancy from 400–500°C, and a rapid increase between 600–800°C as a result of mica and chlorite dehydroxylation. The shape of the dilatometric curve is in accordance with those previously reported in the literature which characterize illite samples [41, 42]. Concerning dilatometric curves of slates, very scarce in the literature, the dilatometric behaviour of the present slate sample up to 900°C is in good agreement with the results reported by Cambronero *et al.* [15].

After heating at 800°C, a first step of sintering seems to take place with a rapid shrinkage (Fig. 4, curve a). From ca. 930°C the dilatometric curve shows an increase in expansion up to ca. 1020°C. This change can be explained by a bloating effect associated to the gas trapped in pores or the release of oxygen gas from the reduction of Fe<sub>2</sub>O<sub>3</sub> [43, 44]. These gases or trapped atmospheric gases expanding in the closed pores with increase in temperature. Finally, the increase in liquid phase by a second step of sintering produces a rapid shrinkage of the slate sample. These thermal changes of expansion-shrinkage can be also observed in the derivative curve (Fig. 4, curve b). The low particle size of the slate sample favours the sintering, but there is also an important factor: the chemical composition. The amount of impurities in this slate (Table 1) suggests the formation of a large proportion of vitreous or liquid phase as increasing temperature. The content of oxides distinct of silica and alumina will form the vitreous phase, which is a liquid after progressive thermal treatments and, hence, it will favour the sintering process. Iron oxide would be the responsible of the bloating effect, as observed by dilatometric analysis (Fig. 4 curve a) in the presence of a liquid phase. In this kind of complex systems,

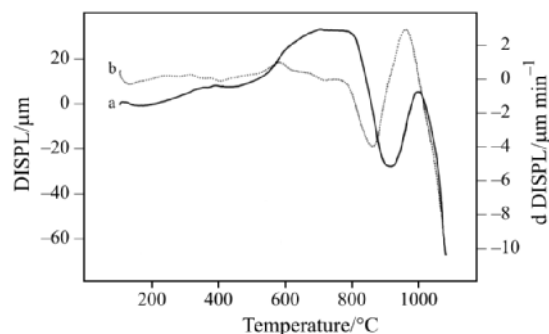
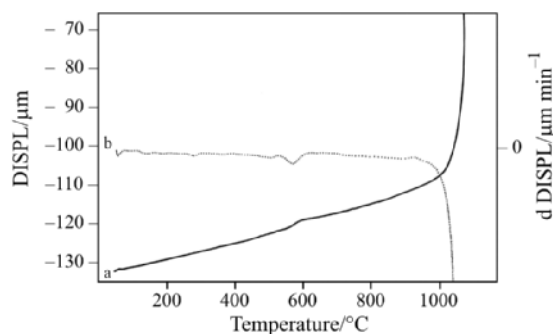


Fig. 4 Dilatometric curves of the original slate sample up to a – 1100°C and the b – derivative curve. Heating rate was 6°C min<sup>-1</sup>

although may be necessary to heat the samples for significantly long period to reach equilibrium, the determination of eutectic temperature is very difficult. According to the SiO<sub>2</sub>–Al<sub>2</sub>O<sub>3</sub>–K<sub>2</sub>O ternary phase diagram at 1 atm pressure [38, 45, 46], the minimum temperature of liquid formation is 985°C. Then, it is clear that a decrease of that temperature and a greater amount of liquid will be produced if different oxides, such as MgO, CaO and Na<sub>2</sub>O (Table 1), are also present. On the other hand, it should be noted that the high amount of iron oxide and the mineralogy, for instance illite, quartz and oligoclase, characterize some raw materials used for ceramics production [47].

Figure 5 shows the dilatometric behaviour of the slate previously heated at 1100°C. It can be thus seen that the only thermal effect recorded in the diagram is the quartz  $\alpha \rightarrow \beta$  phase transition, being more appraised in the derivative curve (Fig. 5, curve b). This dilatometric behaviour is consistent with previous results concerning ceramic raw materials containing quartz after firing [41, 42, 47] and slate samples thermally treated under vacuum, air and N<sub>2</sub>-5% H<sub>2</sub> atmosphere [15].

The XRD patterns at room temperature (original) and after heating the slate sample at 600°C (Fig. 6) show chlorite, mica (illite), quartz and feldspar (microcline), besides the interstratified phase montmorillonite-chlorite. Although there are some little changes in the values of *d*-spacings as compared with those of the original mineral phases, the layered silicate phases observed by XRD at this temperature must be the dehydroxylated phases. Chlorite X-ray patterns disappear after further dynamic heating, which is accounted for in the mass loss (TG-DTG curves, Fig. 3) and the associated endothermal DTA effect (Fig. 3). First of all, there is a decrease in intensity of chlorite X-ray patterns from room temperature to 600–650°C, which coincides with the region of the first endothermal DTA effect centered at 640°C and the DTG peak at 630°C. This is in accordance with



**Fig. 5** Dilatometric curves of the original slate sample after a first thermal treatment at a - 1100°C and b - derivative curve. Heating rate was 6°C min<sup>-1</sup>

the results reported in the literature concerning chlorite thermal transformations [32], where the intensities of the basal reflections are changed markedly by the first stage of reaction, but the spacing is modified only slightly. In a second step, chlorite patterns disappear from 650°C to higher temperatures, which coincides also with the more intense endothermal DTA effect centered at ca. 730°C and the DTG peak at 725°C (Fig. 3). Chlorite X-ray patterns are not present at 800°C. Mica (illite), as a dehydroxylated phase, is observed when the slate sample is being heated (Fig. 6). This phase shows more appraised changes in the range 700–800°C, when the second endothermal DTA effect takes place and the last mass losses are produced (Fig. 3). The interstratified phase montmorillonite-chlorite is not destroyed by heating and it can be observed even at 600°C as a dehydroxylated phase. The X-ray patterns of that phase disappear at 800°C. Quartz is present in the slate sample, but from 600°C the quartz phase must be the  $\beta$ -phase according to its characteristic thermal inversion, as observed previously (Figs 3 and 5). The X-ray patterns of microcline (alkaline feldspar) start to disappear from 800°C (Fig. 6). This is an indication of the formation of a vitreous or liquid phase as increasing the thermal treatment, with progressive incorporation of alkaline ions, as suggested by dilatometry (Fig. 4).

According to the above results, the most important thermal changes of the crystalline phases which constitute the slate sample are evidenced between 600–800°C. Figure 7 shows a more detailed picture concerning these phase changes after dynamic heating. It should be noted that XRD pattern of dehydroxylated mica (zone 25–26 °2 $\theta$ ) does not disappear but changes progressively to coincide with the more intense quartz XRD peak.

Finally, the complete XRD diagram (5–80 °2 $\theta$ ) of Fig. 8 shows the state of the slate sample after dynamic thermal treatment concerning the phase changes up to 1000°C. Dehydroxylated mica can be observed, besides quartz, relicts of microcline and

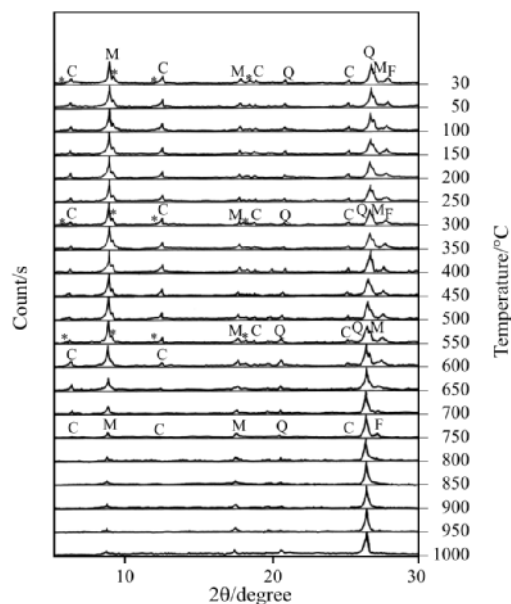


**Fig. 6** XRD powder diagrams in the zone 2 $\theta$ =5–30° corresponding to the original slate sample and after dynamic thermal treatment at several temperatures up to 1000°C. Symbols meaning as in Figs 1 and 2. Note: From 600°C and upper, the layered silicates are identified as crystalline dehydroxylated phases

iron oxide. The observation of dehydroxylated mica at 1000°C is consistent with previous results [33, 38]. The presence of a vitreous or liquid phase in the slate sample after thermal treatment at 1000°C can be inferred from the XRD background because it is amorphous to X-rays (Fig. 8). The disappearance of chlorite (dehydroxylated phase) at 800°C in this slate is in good agreement with the results reported by Rodriguez *et al.* [8] when studying a slate sample containing mainly quartz and, in less proportion, muscovite, chlorite and feldspar. These authors reported also that muscovite is slightly modified and quartz is undranged by thermal treatment, but they considered that this process is exothermic according to their DTA results. The present results on the thermal transformation of a slate sample containing mainly mica (illite), chlorite and quartz demonstrates that the thermal decomposition process of this sample is undoubtedly endothermic (Fig. 3), with changes (expansion) in the dilatometric behaviour (Fig. 4). The previous alteration of muscovite to sericite or illite (considered naturally occurring clay-grade micas) with subsequent particle size reduction can be other factor which would influence the thermal behaviour of the slate, in particular their dehydroxylation process [18, 33, 34, 37, 47, 48].

Returning with previous results on thermal evolution of slates, Cambroneró *et al.* [15] studied the same slate sample previously investigated by García-Guinea *et al.* [17, 18]. The thermal behaviour

## THERMAL EVOLUTION OF A SLATE

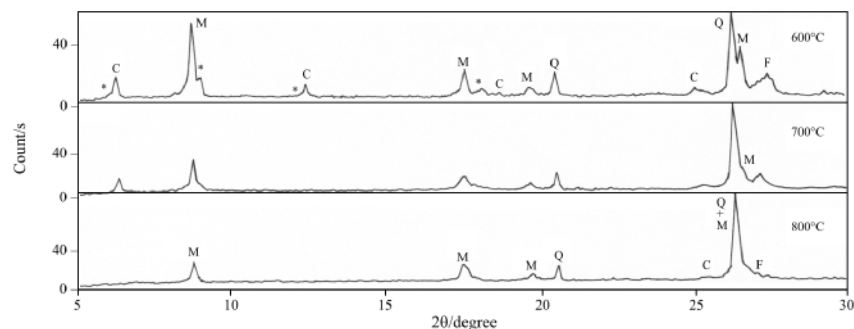


**Fig. 7** XRD powder diagrams in the zone  $2\theta=5\text{--}30^\circ$  corresponding to the slate sample after dynamic thermal treatment at 600, 700 and 800°C. Symbols meaning as in Fig. 1, but from 600°C and upper the layered silicates are identified as crystalline dehydroxylated phases. The presence of a (dehydroxylated) mixed-layer or interstratified phase montmorillonite-chlorite is denoted by asterisks (\*)

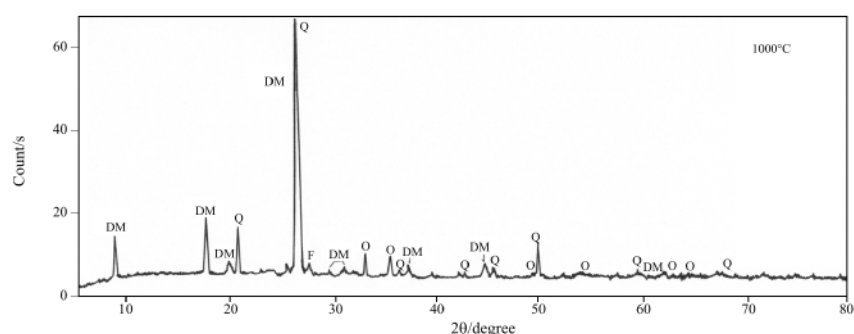


**Fig. 8** XRD powder diagram in the zone  $2\theta=5\text{--}80^\circ$  of a slate sample after thermal treatment at 1000°C using the temperature-controlled device as in Fig. 6. DM is dehydroxylated mica; Q=quartz; F=K-feldspar (microcline); O=iron oxide. Dehydroxylated mica (muscovite): JCPDS file 46-0741

of this slate sample in air, vacuum and  $\text{N}_2\text{--}5\% \text{H}_2$  atmosphere was investigated by dilatometry and XRD after thermal treatments of the sample. These authors emphasized the oxidation or reduction conditions which influence the thermal transformations [15]. Unfortunately, their XRD diagrams were not recorded using dynamic heating conditions. They observed mullite, hercinitite and amorphous silica after heating at 1100°C for 30 min [11, 15]. Heating at 1150°C in air produced mullite, hematite, spinel-like phases (hercinitite), quartz and alumina, and above 1200°C, the crystalline phases detected by XRD are quartz, mullite and hercinitite [11, 15]. However, the same authors reported the formation of hieratite ( $\text{K}_2\text{SiF}_6$ ) with presence of quartz after sintering at 1150°C for 30 min in  $\text{N}_2\text{--}5\% \text{H}_2$  atmosphere. These authors claimed that the formation of hieratite can be produced from the thermal decomposition of muscovite, with composition  $\text{KAl}_2(\text{Si}_3\text{Al})\text{O}_{10}(\text{OH},\text{F})_2$  which they identified in the sample slate. It should be remarked that Rodríguez *et al.* [8], studying other slate sample, found the presence of secondary minerals like pyrite, hematite and goethite. These secondary minerals could influence the thermal behaviour of the slate [49, 50]. In this sense, Decler and Viaene [48] have previously discussed the thermal reactions in a

raw clay material containing pyrite and carbon. On the other hand, it should be noted that the presence of illite and/or chlorite as dehydroxylated phases, could be used to evaluate the possible firing temperature of a ceramic sample [51].

The above results emphasize that the thermal behaviour of slate samples can be very complex according to the original mineral phases and the conditions of thermal treatment. The problem will be more difficult considering the particle size, chemical composition (especially impurities) and the thermodynamic equilibria in this kind of systems [46, 49, 50]. In the present case, however, the thermal behaviour of a particular slate sample in air up to 1000°C has been investigated using thermoanalytical techniques, in particular thermal diffractometry under dynamic conditions of heating as an approach to study the phase transformations.

## Conclusions

In this investigation, the thermal evolution of a slate sample has been studied. The main minerals identified by XRD were mica (illite), chlorite (clinocllore) and quartz, with minor interstratified phase (montmorillonite-chlorite), microcline (K-feldspar) and iron oxide. The

particle size distribution allowed to calculate an average particle size of 23  $\mu\text{m}$  in samples sieved under 100  $\mu\text{m}$  (ca. 80 mass% of the total). The chemical composition of the slate is highly silico-aluminous, with 48.33 mass% silica and 22.04 mass% alumina. The content of other elements as oxides is ca. 20 mass% of the total chemical composition, in particular iron, alkaline-earths and alkaline oxides. These results are in well agreement with the mineralogical composition. Although interlayer cations must be also present in the structure of layered silicates, the alkaline oxides are associated to illite and microcline.

Thermal analysis of the slate sample by DTA-TG and dilatometry confirmed the mineralogical composition. The thermal behaviour was interpreted considering the structure of 2:1 layered silicates assuming: (1) a first step of dehydroxylation of brucite-like layers of chlorite (clinochlore) at ca. 640°C, and (2) a second step of dehydroxylation of 2:1 talc-like layers of this silicate at ca. 730°C, which is overlapped with the dehydroxylation of illite, with octahedrally coordinated cations (gibbsite), besides the dehydroxylation of the interstratified phase. In consequence, mass loss is larger in the second step (4.14 mass%) and the DTA and DTG effects are more intense than those observed at the first step. The dehydroxylation of the layered silicates has been also evidenced by dilatometry, with a rapid increase of expansion between 600–800°C, and upper 800°C the first sintering effects associated to a shrinkage of the sample. The sintering process is also favoured by the low particle size of the sample and the presence of a liquid or vitreous phase which can easily be formed taking into account the chemical composition of the sample (Table 1). An increase in expansion up to ca. 1020°C was interpreted by a bloating effect. This effect is caused by gas trapped in the pores and the release of oxygen gas, the last being characteristic of raw materials containing iron oxides. The presence of free quartz was detected by DTA (original slate sample) and dilatometry (after a previous heating of the sample up to 1100°C) according to its characteristic  $\alpha \rightarrow \beta$  thermal phase transition at 573°C.

The application of thermal diffractometry has allowed the examination of the thermal behaviour of slate under dynamic conditions of heating. It has been thus confirmed by XRD the formation of dehydroxylated crystalline phases from layered silicates after heating, with slight differences in their XRD patterns as compared with the original (hydroxylated) layered silicates present in the mixture. Chlorite (clinochlore), as dehydroxylated phase previously formed at ca. 600°C, disappear from 650°C to higher temperatures, being not present at ca. 800°C. The formation of dehydroxylated illite was also

evidenced. This crystalline phase showed some changes at 700–800°C, when the more intense DTA and DTG peaks are observed. The interstratified phase montmorillonite-chlorite, present as dehydroxylated phase at ca. 600°C, disappears at 800°C. The progressive disappearance of microcline from 800°C is associated to an increase of vitreous or liquid phase by heating, which is in well agreement with the dilatometric behaviour. At 1000°C,  $\beta$ -quartz, dehydroxylated illite, iron oxide, relicts of microcline and the vitreous phase are present.

The present investigation has allowed to know the main changes associated to the thermal transformations of a slate sample constituted by a mineral mixture of several layered silicates and a mixed layer or interstratified phase. Although the mineral mixtures of slate samples can be very complex, and the reported results on the thermal evolution of slate samples are very scarce, the results of this paper have provided a better understanding of the thermal behaviour of slates with a previous characterization.

## Acknowledgements

Financial support by Spanish Ministry of Education and Science, Research Project CTQ2005-998 cofinanced with Feder, is gratefully acknowledged. This paper is dedicated to the memory of Professor and friend Dr. Joaquín Rivas Florido, recently deceased in Utrera (Sevilla, Spain).

## References

- 1 H. G. F. Winkler, *Petrogenesis of Metamorphic Rocks*, Springer Verlag, 1976.
- 2 P. Sousa Santos, *Tecnologia de argilas aplicada as argilas brasileiras*, Vol. 2, p. 148, Blücher Ltd., Sao Paulo (Brasil) 1975.
- 3 D. S. Woods, Current views of development of slaty cleavage, *An. Rev. Earth Sci.*, 2 (1974) 1.
- 4 R. L. Bates and J. A. Jackson, *Glossary of Geology*, Am. Geol. Inst., 1987.
- 5 W. A. Deer, R. A. Howie and J. Zussman, *An Introduction to the Rock-forming Minerals*, Longman, Hong Kong 1992.
- 6 Anon, What is slate?, *Altivopedras Company*, Minas Gerais, Brazil 2002, in [www.altivopedras.com](http://www.altivopedras.com).
- 7 M. Lombardero and J. M. Quereda, *Recursos minerales de España*, Textos Universitarios, J. García and J. Martínez, Eds., CSIC, Madrid, Spain 1992, pp. 1118–1150.
- 8 M. A. Rodríguez, F. Rubio, J. Rubio, M. J. Liso and J. L. Oteo, *Bol. Geol. Min.*, 106 (1995) 437.
- 9 M. A. Rodríguez, J. Rubio, F. Rubio, M. J. Liso and J. L. Oteo, *Clays Clay Miner.*, 45 (1997) 670.
- 10 T. U. Pritchard, *Development of Expanded Slate for Horticultural and Aggregate Use*, Eurothen 2000, Lisbon, 19–21 January 2000.
- 11 M. T. Vieira, L. Catarino, M. Oliveira, J. Sousa, J. M. Torralba, L. E. G. Cambronero,

- F. L. González-Mesones and A. Victoria, *J. Mater. Process. Technol.*, 92–93 (1999) 97.
- 12 R. Caligaris, N. Quaranta, M. Caligaris and E. Benavides, *Bol. Soc. Esp. Ceram. V.*, 39 (2000) 623.
  - 13 M. Regueiro and M. Lombardero, *Innovaciones y avances en el sector de las rocas y minerales industriales*, Summa S.A., Madrid 1997.
  - 14 T. S. Valera, A. P. Ribeiro, F. R. Valenzuela-Díaz, A. Yoshiga, W. Ormanji and S. M. Toffoli, *Annual Technical Conference-Society of Plastics Engineers*, 3 (2002) 3949.
  - 15 L. E. G. Cambronero, J. M. Ruiz-Román and J. M. Ruiz, *Bol. Soc. Esp. Ceram. V.*, 44 (2005) 368.
  - 16 J. Garcia-Guinea, M. Lombardero, B. Roberts and J. Taboada, *Trans. Inst. Min. Metall. (Sect. B: Appl. Earth Sci.)*, 106 (1997) 205.
  - 17 J. Garcia-Guinea, M. Lombardero, B. Roberts, J. Taboada and A. Peto, *Mater. Construcc.*, 48 (1998) 37.
  - 18 J. Garcia-Guinea, V. Cardenas, V. Correcher, A. Delgado, M. Lombardero and J. C. Barros, *Bol. Soc. Esp. Ceram. V.*, 39 (2000) 589.
  - 19 B. A. van der Pluijm, N.-C. Ho, D. R. Peacor and R. J. Merriman, *Nature*, 392 (1998) 348.
  - 20 M. A. Rodríguez, F. Rubio, J. Rubio, M. J. Liso and J. L. Oteo, *Bol. Soc. Esp. Ceram. V.*, 40 (2001) 101.
  - 21 E. Garzon, A. Ruiz-Conde and P. J. Sanchez-Soto, *Communication presented at VIII Congreso Nacional de Materiales*, Valencia 2004.
  - 22 P. J. Sánchez-Soto, M. C. Jiménez de Haro, L. A. Pérez-Maqueda, I. Varona and J. L. Pérez-Rodríguez, *J. Am. Ceram. Soc.*, 83 (2000) 1649.
  - 23 G. W. Brindley and G. Brown, *Crystal structures of clay minerals and their X-ray identification*, Mineralogical Society, London 1980.
  - 24 S. W. Bailey and J. S. Lister, *Clays Clay Miner.*, 37 (1989) 193.
  - 25 D. M. C. MacEwan and A. Ruiz-Amil, *Interstratified Clay Minerals, Soil Components, Vol. 2, Inorganic Components*, J. E. Gieseking Ed., Springer-Verlag, New York, 1975, pp. 265-334.
  - 26 A. Ruiz-Amil, F. Aragón, E. Vila and A. Ruiz-Conde, *Clay Miner.*, 27 (1992) 257.
  - 27 A. Ruiz-Conde, A. Ruiz-Amil, J. L. Pérez-Rodríguez and P. J. Sánchez-Soto, *J. Mater. Chem.*, 6 (1996) 1557.
  - 28 A. Ruiz-Conde, E. Garzón and P. J. Sánchez-Soto, *in preparation*.
  - 29 A. Justo, J. L. Pérez-Rodríguez and P. J. Sánchez-Soto, *J. Therm. Anal.*, 40 (1993) 59.
  - 30 K. H. Schüller, *Process Mineralogy of Ceramic Materials*, Ed. W. Baumgart *et al.*, pp. 1–27, Ferdinand Enke, Stuttgart, Germany 1984.
  - 31 G. W. Brindley and T. S. Chang, *Am. Miner.*, 59 (1974) 152.
  - 32 G. W. Brindley and J. Lemaitre, *Chemistry of Clays and Clay Minerals* A. C. D. Newman Ed., Monograph No. 6, The Mineralogical Society, London 1987, p. 319.
  - 33 H. Takeda and B. Morosin, *Acta Crystall.*, B31 (1975) 2444.
  - 34 S. Guggenheim, Y. H. Chang and A. F. Koster van Groos, *Am. Miner.*, 72 (1987) 537.
  - 35 K. J. D. MacKenzie, I. W. M. Brown, C. M. Cardile and R. H. Meinhold, *J. Mater. Sci.*, 22 (1987) 2645.
  - 36 E. Murad and U. Wagner, *Clay Miner.*, 31 (1996) 45.
  - 37 G. E. Roch, M. E. Smith and S. R. Drachman, *Clays Clay Miner.*, 46 (1998) 694.
  - 38 S. G. Barlow and D. A. C. Manning, *Br. Ceram. Trans. J.*, 98 (1999) 122.
  - 39 S. W. Bailey, *Structures of Layer Silicates*, in [23], p. 1.
  - 40 A. F. Koster van Groos and S. Guggenheim, in *CMS Workshop Lectures, Vol. 3, Thermal Analysis in Clay Science*, J. W. Stucki, D. L. Bish and F. A. Mumpton eds., The Clay Minerals Society, Boulder, Colorado, 1990, p. 49.
  - 41 P. Munier and J. Meneret, *Bull. Soc. Fr. Ceram.*, 7 (1950) 6.
  - 42 G. García Ramos, F. González García, P. J. Sánchez-Soto and M. T. Ruiz, *Bol. Soc. Esp. Ceram. V.*, 24 (1985) 67.
  - 43 M. S. Tites and Y. Maniatis, *Br. Ceram. Trans. J.*, 74 (1975) 19.
  - 44 A. W. Norris, D. Taylor and I. Thorpe, *Br. Ceram. Trans. J.*, 78 (1979) 102.
  - 45 J. F. Schairer, *J. Am. Ceram. Soc.*, 40 (1957) 215.
  - 46 E. F. Osborn and A. Muan Eds., *Phase diagrams for ceramists, Plate 407*, The American Ceramic Society, Columbus, Ohio 1960.
  - 47 V. Nastro, D. Vuono, M. Guzzo, G. Nicéforo, I. Bruno and P. De Luca, *J. Therm. Anal. Cal.*, 84 (2006) 181.
  - 48 D. D. Eberl and J. Shrodon, *Am. Miner.*, 73 (1988) 1335.
  - 49 J. Decler and W. Viaene, *Appl. Clay Sci.*, 8 (1993) 111.
  - 50 A. Muan, *J. Am. Ceram. Soc.*, 40 (1957) 121.
  - 51 D. N. Papadopoulou, M. Lalia-Kantouri, N. Kantiranis and J. A. Stratis, *J. Therm. Anal. Cal.*, 84 (2006) 39.

---

Received: June 26, 2006

Accepted: April 12, 2007

OnlineFirst: July 11, 2007

---

DOI: 10.1007/s10973-007-7751-2